ARTICLE

Spatial and temporal dynamics of HDACs class IIa following mild traumatic brain injury in adult rats

Swatabdi R. Kamal[1], Shreya Potukutchi[1], David J. Gelovani[2], Robin E. Bonomi[2], Srinivasu Kallakuri[3], John M. Cavanaugh[1], Thomas Mangner[4,5], Alana Conti[6,7], Ren-Shyan Liu[8,9,10], Renata Pasqualini[5,11], Wadih Arap[11,12], Richard L. Sidman[13], Shane A. Perrine[3] and Juri G. Gelovani[1,14,15]✉

The fundamental role of epigenetic regulatory mechanisms involved in neuroplasticity and adaptive responses to traumatic brain injury (TBI) is gaining increased recognition. TBI-induced neurodegeneration is associated with several changes in the expression-activity of various epigenetic regulatory enzymes, including histone deacetylases (HDACs). In this study, PET/CT with 6-([^{18}F] trifluoroacetamido)−1- hexanoicanilide ([^{18}F]TFAHA) to image spatial and temporal dynamics of HDACs class IIa expression-activity in brains of adult rats subjected to a weight drop model of diffuse, non-penetrating, mild traumatic brain injury (mTBI). The mTBI model was validated by histopathological and immunohistochemical analyses of brain tissue sections for localization and magnitude of expression of heat-shock protein-70 kDa (HSP70), amyloid precursor protein (APP), cannabinoid receptor-2 (CB2), ionized calcium-binding adapter protein-1 (IBA1), histone deacetylase-4 and −5 (HDAC4 and HDAC5). In comparison to baseline, the expression-activities of HDAC4 and HDAC5 were downregulated in the *hippocampus*, *nucleus accumbens*, peri-3rd ventricular part of the thalamus, and *substantia nigra* at 1–3 days post mTBI, and remained low at 7–8 days post mTBI. Reduced levels of HDAC4 and HDAC5 expression observed in neurons of these brain regions post mTBI were associated with the reduced nuclear and neuropil levels of HDAC4 and HDAC5 with the shift to perinuclear localization of these enzymes. These results support the rationale for the development of therapeutic strategies to upregulate expression-activity of HDACs class IIa post-TBI. PET/CT (MRI) with [^{18}F] TFAHA can facilitate the development and clinical translation of unique therapeutic approaches to upregulate the expression and activity of HDACs class IIa enzymes in the brain after TBI.

Molecular Psychiatry (2022) 27:1683–1693; https://doi.org/10.1038/s41380-021-01369-7

INTRODUCTION

Traumatic brain injury (TBI) is a major health problem worldwide, contributing to severe disability and substantial mortality. Mild TBI (mTBI) affects between 1.8 and 3.5 million people each year in the United States alone, with 20% of those subjects developing chronic disabilities [1]. Moderate-to-severe traumatic brain injury (msTBI) affects about half a million individuals per year and accounts for one-third of all injury-related deaths [1]. Many individuals with TBI develop diverse physical, neurological and psychiatric co-morbidities including post-traumatic stress disorder (PTSD), along with various affective, anxiety, personality, or behavior disorders, and even schizophrenia [2, 3]. Furthermore, many of the 1.6 million US personnel deployed since 2001 as part of various military operations in Iraq and Afghanistan have sustained brain concussions, with most of them being blast related [4, 5]. These service members often have other psychological co-morbidities such as depression, anxiety, somatoform disorders, and substance abuse [6–11]. With the wide-ranging socio-economic impact of TBI and associated co-morbidities, an improved understanding of mechanisms involved in its molecular pathophysiology will facilitate the development of more effective and/or creative therapeutic solutions.

Even though the various physical and behavioral abnormalities cited above in humans involve neurons, glia, inflammatory cells, and microvasculature [12–14], in this study, we have focused essentially on neuronal cell bodies. Here we used a model of mTBI on adult rats, which is known to cause diffuse neuronal injury without either focal contusion or hemorrhage. Our immunohistochemical and radiological analyses demonstrate the upregulation of biomarkers of neuronal stress and

[1]Department of Biomedical Engineering, College of Engineering and School of Medicine, Wayne State University, Detroit, MI 48201, USA. [2]School of Medicine, Wayne State University, Detroit, MI 48201, USA. [3]Department of Psychiatry and Behavioral Neurosciences, School of Medicine, Wayne State University, Detroit, MI 48201, USA. [4]Cyclotron-Radiochemistry Facility, Karmanos Cancer Institute, Wayne State University, Detroit, MI 48201, USA. [5]Division of Cancer Biology, Department of Radiation Oncology, Rutgers New Jersey Medical School, Newark, NJ 07103, USA. [6]Research and Development Service, John D. Dingell VA Medical Center, Detroit, MI 48201, USA. [7]Departments of Neurosurgery and Psychiatry and Behavioral Neurosciences, Wayne State University School of Medicine, Detroit, MI 48201, USA. [8]Department of Biomedical Imaging and Radiological Sciences, National Yang Ming Chiao Tung University, Taipei 112, Taiwan. [9]Department of Nuclear Medicine, Cheng-Hsin General Hospital, Taipei 112, Taiwan. [10]Department of Nuclear Medicine, Taipei Veterans General Hospital, Taipei 112, Taiwan. [11]Rutgers Cancer Institute of New Jersey, Newark, NJ 07103, USA. [12]Division of Hematology/Oncology, Department of Medicine, Rutgers New Jersey Medical School, Newark, NJ 07103, USA. [13]Department of Neurology, Harvard Medical School, Boston, MA 02115, USA. [14]Molecular Imaging Program, Karmanos Cancer Institute, Wayne State University, Detroit, MI 48201, USA. [15]College of Medicine and Health Sciences, United Arab Emirates University, Al Ain, Abu Dhabi, UAE. ✉email: jgelovani@uaeu.ac.ae

Received: 9 May 2021 Revised: 28 September 2021 Accepted: 15 October 2021
Published online: 14 January 2022

damage, as well as of reactive microglia at acute and subacute intervals post-trauma.

Over the past decade, the importance of epigenesis in the pathophysiology of TBI has been gaining increased recognition [15, 16]. Epigenetic regulatory mechanisms include DNA methylation, histone modifications (i.e., acetylation, methylation), post-transcriptional regulation of gene expression via small noncoding RNAs, and post-translational modifications of various structural and signaling proteins that impact their stability and function [17, 18]. Histone deacetylases (HDACs) play central functional roles in epigenetic regulation [17, 18]. Several HDAC isoforms are responsible for the regulation of gene transcription by the removal of acetyl moieties from the acetylated lysine residues of histone core proteins, and thereby increases DNA binding to histones, ultimately resulting in transcriptional repression [19]. HDACs have 18 known isoforms divided into four classes, namely: class I (HDACs 1, 2, 3, and 8), IIa (HDACs 4, 5, 7 and 9), class IIb (HDACs 6 and 10), class III or sirtuins (SIRTs 1–7) and class IV (HDAC11) [20]. Disruption of acetylation/deacetylation of histone core proteins and other non-histone proteins is a common feature in various diseases and neuropathological states [21, 22]. It has been demonstrated that neurodegeneration is associated with a global decrease in histone acetyl-transferase activity resulting in an abundance of deacetylated histones [23, 24]. Furthermore, there is growing awareness of the neuroprotective effects of some HDAC inhibitors [25]. Valproic acid, an inhibitor of HDACs class I, exhibits neuroprotective effects in rodent models of TBI by decreasing blood–brain barrier (BBB) permeability, reducing neuronal damage, plus improving motor function and spatial memory [26]. DMA-PB, an HDAC6 (class IIb) inhibitor [27], increases histone H3 acetylation and reduces the microglial inflammatory response in a unilateral fluid percussion TBI model in rats [28]. ACY-1083, another HDAC6 (class IIb) inhibitor, reduces traumatic lesion size and brain edema in a swine model of severe TBI with hemorrhagic shock [29]. Givinostat (ITF2357), a pan-HDAC inhibitor [30], substantially improves the long-term recovery of several neurological functions in a mouse model of closed TBI [31].

Moreover, Scriptaid, an HDAC class I and IIb inhibitor, promotes the resolution of hematoma and brain edema and alleviates neurological dysfunction after an experimental intracerebral hemorrhage in mice [32] and induces a neuroprotective effect by modulating the microglia/macrophage polarization through the glycogen synthase kinase-3-β (GSK3β)/PTEN/AKT pathway after a controlled cerebral cortical impact [33, 34]. Similarly, the pan-HDAC inhibitor LB-205 induces potent neuroprotective effects by preserving nerve growth factor (NGF)-mediated cell survival flowing TBI in rats [35]. Other studies revealed that pan-HDAC inhibitors augment memory, synaptic plasticity, and promote neuronal outgrowth [36–38]. Surprisingly, however, a comprehensive study of a structurally diverse panel of HDAC inhibitors revealed an unexpected isoform selectivity of these so-called "pan-HDAC inhibitors" for the HDAC class I, and to a lesser degree for the HDACs class IIb, but not the HDACs class IIa or classes III enzymes [39]. Therefore, the mechanism of neuroprotection observed with such drugs could be largely attributed to the inhibition of HDACs class I and IIb enzymes.

In contrast to the well-studied roles of HDACs class I and IIb in TBI and the neuroprotective effects resulting from their pharmacologic inhibition, the roles of HDACs class IIa enzymes in the pathophysiology of TBI have not as yet been sufficiently established. The importance of HDACs class IIa in epigenetic mechanisms of TBI is evidenced by studies in mice deficient in HDAC4, 5, and 9, which exhibit impaired neuroplasticity [40], reduced axonal regeneration [41] along with defects in spatial learning and memory [42, 43]. Thus, class IIa HDACs seems to play considerable roles in the pathophysiology of different neurological diseases or conditions resulting from TBI.

Recently, it has been demonstrated that in a controlled cerebral cortical impact mouse model, TBI causes degradation and downregulation of HDAC4 activity, which elicits post-traumatic psychiatric disorders through impairment of neurogenesis [44], whereas the overexpression of HDAC4 in the hippocampus by plasmid-mediated transfection pre-TBI restores neurogenesis, reduces anxiety and depressive-like behavior, and improves memory functions post-TBI. In contrast, another recent study [45] with a weight drop model of repeated mTBI in adult rats demonstrates that the compromised hippocampal recognition memory was associated with a clear upregulation of HDAC4 and HDAC5 mRNA levels and hypoacetylation of histones in hippocampal neurons during both, at 48 h and 30 days post mTBI. The latter study has also shown that treatment with trichostatin (TSA) leads to both, recovered hippocampal learning and memory deficit. Thus, there is an ongoing controversy and debate regarding the levels of HDACs class IIa expression-activity in the brain following TBI, especially in terms of the levels of TBI severity and post-traumatic phases.

To address this open question experimentally, we have conducted studies by using non-invasive in vivo PET/CT imaging with HDAC class IIa-specific substrate-type radiotracer 6-(trifluoroacetamido)−1-hexanoicanilide ([^{18}F]TFAHA) [46] to quantitatively visualize the spatial and temporal dynamics of HDAC class IIa expression-activity in the rat brain during early phases post TBI. Our results support the rationale for the future development of therapies of TBI targeted to HDACs class IIa expression and activity in the brain.

MATERIALS AND METHODS

Animal study groups

All procedures were approved by the Institutional Animal Care and Use Committee (Wayne State University). Male Sprague-Dawley rats (n = 16; 250–300 g, Envigo, MI) were used in this study. One group of rats ($n = 13$) was subjected to a diffuse mTBI, another group of rats ($n = 3$) underwent a sham (negative control) procedure. PET/CT imaging with [^{18}F]TFAHA was performed in 7 rats at baseline (before mTBI), 1–3 days post mTBI, and 7–8 days post mTBI. In parallel, nine rats ($n = 3$ per time point) were euthanized for histologic and immunohistochemical analyses of brain tissue sections. No randomization was used in this study. Investigators were not blinded to the group allocation and when assessing the outcome.

Mild diffuse traumatic brain injury model

Mild diffuse TBI was induced using the Marmarou impact-acceleration model, which has been reported extensively elsewhere [47–66]. Briefly, 30 min before induction of mTBI, the rats were pretreated with buprenorphine (0.3 mg/kg, subcutaneously). Then, anesthesia was induced by 4% isoflurane in oxygen and maintained with 2% isoflurane in oxygen (0.6 L/min). A midline incision was made to expose the skull. A stainless-steel disk (diameter 10 mm, thickness 3 mm) was subsequently secured midline between *bregma* and *lambda* with cyanoacrylate glue. Next, the rat was placed prone on an open-cell flexible polyurethane foam bed (12 × 12 × 43 cm; Foam to Size Inc., Ashland, VA) contained in a plexiglass box. The animals were further immobilized by taping over their trunk. The head of each rat was then positioned with the stainless-steel disk centered under the lower end of an acrylic tube (2.5 m long, 57 mm diameter) and a custom-made 450 g impactor was dropped through the tube from a height of 1 m (calculated impact velocity of 4.43 m/s). Following the impact, the stainless-steel disk was removed and the animals without skull fracture had their scalp sutured (4.0 silk) and allowed to recover. The sham group of animals underwent all the same procedures except for the impactor drop.

PET/CT imaging with [^{18}F]TFAHA

The radiolabeling of [^{18}F]TFAHA was performed as described in detail previously [46]. The rats were anesthetized with 4% isoflurane in oxygen and maintained with 2% isoflurane in oxygen (0.6 L/min) throughout the imaging procedure with the body temperature being maintained with an electronically controlled heating pad (M2M Imaging, Cleveland, OH) set at 37 °C. The rats were placed in the supine position on the bed of microPET

R4 scanner (Siemens, Knoxville, TN) with the head in the center of the field of view (FOV) and then [^{18}F]TFAHA (300–500 μCi/animal in 1 ml of saline) was administered via the tail-vein as a slow bolus injection over 1 min. Then, dynamic PET images were acquired over a 30-min time. After PET imaging, the bed with the affixed anesthetized animal was transferred to the Inveon SPECT/CT scanner (Siemens, Knoxville, TN) and CT images were acquired with four overlapping frames (2 min each) covering the whole body, with X-ray tube settings of 80 kV and 500 μA. PET images were reconstructed using the ordered subset expectation–maximization method [67]. Digital Rat Brain Atlas was used for the alignment and identification of specific anatomical markers in the brain [68]. The levels of [^{18}F]TFAHA accumulation in different regions of the brain were measured by using AMIDE 1.0.4 image analysis software and expressed as standard uptake values (SUV) [69]. The volume of distribution (VD) of [^{18}F]TFAHA in different brain structures was calculated using Logan graphical analysis [46, 67, 69–71] with frontal cortex as the reference tissue [46, 72].

Histology and immunohistochemistry

Rats were euthanized with an overdose of sodium pentobarbital (50 mg/kg intravenously (i.v.) and then transcardially perfused with normal saline followed by 4% formaldehyde in phosphate-buffered saline (PBS 0.1 M, pH 7.4) until completely exsanguinated. The brain was extracted and postfixed in 4% formaldehyde with 30% sucrose for 2 days, followed by storage in 30% sucrose in PBS. Subsequently, frozen brain sections (20 μm) were obtained in a coronal plane (OTF5000 cryomicrotome, Hacker-Bright), dried at 55 °C on a slide warmer, and then stored at −80°C. For immunohistochemistry, the brain sections were washed in 0.1 M PBS (pH 7.4) 3 × 3 min and processed for antigen retrieval by incubating the sections at 75 °C in sodium citrate buffer (pH 6.0) for 1 h, followed by washing in PBS 3 × 3 min and blocking the endogenous peroxidase activity with 0.6% hydrogen peroxide in PBS for 1 h. Then, the sections were rinsed in PBS 3 × 3 min and incubated overnight (ON) with one of the primary antibodies: HDAC4 H-92 (1:100, Santa Cruz Biotechnology), HDAC5 H-64 (1:100, Santa Cruz Biotechnology), HSP70 (1:1000, Enzo Life Science), CB2 (1:500, Enzo Life Science), or β-APP (1:1000, Life Technologies),. The next day, the sections were washed in PBS 3 × 3 min, incubated with goat anti-rabbit biotinylated secondary antibody (Vectastain ABC Kit, Vector Laboratories) for 1.5 h, washed in PBS 3 × 3 min, and then incubated for 1 h with avidin-peroxidase complex solution (Vector Laboratories). After washing 3 × 10 min with PBS, the sections were incubated for 90 s in a water solution containing 0.05% 3,3-diaminobenzidine and 0.015% H_2O_2 (Sigma Aldrich), gently washed in tap water, counterstained with hematoxylin and coverslipped with Surgipath Micromount medium (Leica). The images of stained brain sections were acquired with a digital microscope EVOS FL Auto (Life Technologies).

Quantification of HDAC4 and HDAC5 expression in situ

The magnitude of expression of HDAC4 and HDAC5 in IHC-stained rat brain sections was quantified by densitometric analysis using ImageJ software (https://imagej.nih.gov/ij). The number of neurons showing no staining (null), only nuclear, only cytoplasmic, or both nuclear and cytoplasmic (dual) staining for HDAC4 and HDAC5 were counted by two independent observers and expressed as a percentage (%) of the total number of neurons per FOV, and the mean ± standard error of the mean (SEM) values was calculated. The nuclear and corresponding cytoplasmic optical density (OD) of staining of HDAC4 or HDAC5 was measured in individual neurons to calculate the cytoplasmic over nuclear OD ratio (minimum $N = 36$/FOV). Calculating the ratio of nuclear to cytoplasmic staining intensity cancels out the small differences in absolute levels of staining intensity between different cells, different sections, and different animals.

Statistical analyses

Numerical and statistical analyses of data were performed with Excel 2013 (Microsoft, Redmond, WA) and Graph-Pad Prism 6 (Graph Pad Software La Jolla, CA). The adequacy of numbers of animals per group per time point (sample size) was determined by power analysis using *F*-tests, one-way ANOVA ($\alpha = 0.05$; power = 0.80). Group means ± SEM were calculated for SUVs and VD in different brain structures (i.e., *hippocampus*, *n.accumbens*, *substantia nigra*, and peri-3rd ventricular part of *thalamus*) at baseline and different phases post mTBI and compared by using one-way ANOVA for repeated measures in the same subjects. Student *t*-tests for group mean and paired measurements were performed to calculate *p* values, an α of 0.05 was used as the threshold to indicate a significant difference, and a two-tailed distribution was assumed; $p < 0.05$ was considered statistically significant.

RESULTS

IHC characterization of mTBI model

At 6 h post mTBI, rats subjected to brain trauma had a markedly increased expression of HSP70, β-APP, and CB2 in neurons of the hippocampal CA1, CA2, CA3 regions, dentate gyrus, and in cerebral cortical pyramidal neurons. In contrast, these biomarkers of brain injury remained at low to non-detectable levels in rats that underwent a control sham procedure (Figs. S1–S9). Also, at 6 h post mTBI increased expression of the ionized calcium-binding adapter molecule-1 (IBA1) was observed in the activated microglial cells throughout the CA1, CA2, CA3 regions of the hippocampus and its dentate gyrus, and cortex, in comparison to the brain in rats that underwent the control sham procedure (Figs. S10–S12).

PET/CT Imaging with [^{18}F]TFAHA

The spatial and temporal dynamics of HDACs class IIa activity in different structural regions of the rat brain were quantified using PET/CT with [^{18}F]TFAHA at baseline, 1–3 days, and 7-8 days post mTBI (Fig. 1). There were no significant differences ($p > 0.1$) in [^{18}F]TFAHA SUVs between 1 and 3 days post mTBI and, therefore, the data were pooled. However, as compared to baseline, at 1–3 days post mTBI a significant decrease in [^{18}F]TFAHA SUV ($p < 0.001$) and VD ($p < 0.05$) was observed in the part of the thalamus around the third (3rd) ventricle (Fig. 1, row 4), *n. accumbens, hippocampus (row 3)*, and *substantia nigra* (row 2) (see also Figs. 2, S13, and S14). At 7-8 days post mTBI, the levels of [^{18}F]TFAHA-derived radioactivity accumulation in these brain regions, as measured by SUV, were significantly higher ($p < 0.01$) than in the acute phase (1–3 days) post mTBI, and were similar to baseline levels. Although the VD of [^{18}F]TFAHA in these brain regions showed a tendency to increase, as compared to the acute phase (1–3 days post mTBI), it remained significantly lower ($p < 0.05$) than the baseline levels (Figs. 1, 2, S13, and S14).

HDAC4 expression in neurons

At baseline, higher levels of HDAC4 expression were observed in neurons of *hippocampus*, *peri-3rd ventricular thalamic nuclei*, *n. accumbens*, and *substantia nigra*, as compared to other regions of the brain (Figs. 3, 4, S15–S17). The intracellular localization of HDAC4 expression in neurons of these regions was both cytoplasmic and nuclear (dual), as evidenced by the predominant percentage of dual-stained neurons (Fig. S18). However, the nuclear levels of HDAC4 expression were higher in the nuclei than in the cytoplasm, as evidenced by the low (below 1) cytoplasmic-to-nuclear OD ratio (Fig. 6A). During days 1–3 post mTBI, the overall level of HDAC4 expression in neurons of these regions was reduced (Figs. 3, S15–S17), while the intracellular localization of HDAC4 expression was shifted predominantly into the cytoplasm, as evidenced by the significantly increased ($p < 0.05$) percentage of only cytoplasm-stained neurons (Fig. S18) and increased cytoplasmic-to-nuclear OD ($p < 0.01$) (Fig. 6A), as compared to baseline levels. During the 7–8 days post mTBI, the overall level of HDAC4 expression in neurons of these regions remained lower than baseline but showed a tendency to increase over the levels observed at 1–3 days post mTBI (Figs. 3, S15–S17). However, the intracellular localization of HDAC4 expression at 7–8 days post mTBI was further shifted to the cytoplasm, as evidenced by the significantly increased ($p < 0.05$) percentage of only cytoplasm-stained neurons (Fig. S18) and increased cytoplasmic-to-nuclear OD (Fig. 6A), as compared to baseline and 1–3 days post mTBI ($p < 0.01$). No other regions of the brain with these pathological changes were noted.

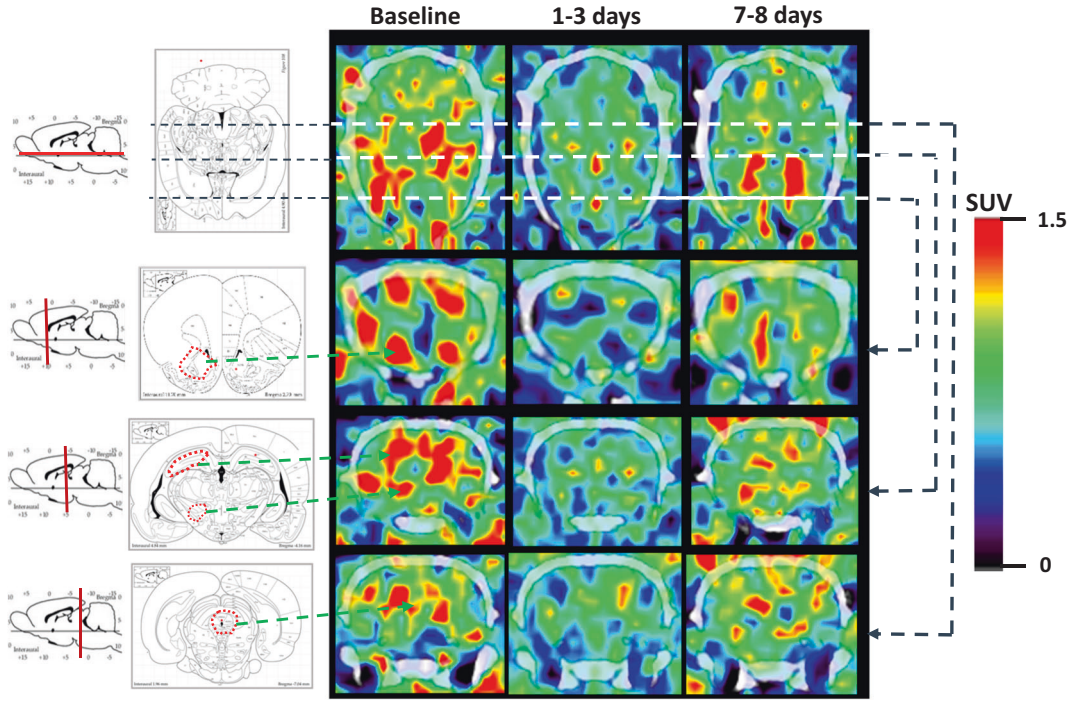

Fig. 1 PET/CT images of the rat brain at 20–30 min post [^{18}F]TFAHA administration obtained at baseline, 1–3 days, and 7–8 days post-TBI. Axial images (top row) and coronal images (lower three rows) reflect [^{18}F]TFAHA accumulation (Standard uptake values; SUV) in the following brain structures outlined by the red dots: *n. accumbens* (row 2), *hippocampus* and *substantia nigra* (row 3), and *peri-3rd ventricular thalamic gray matter* (row 4). The corresponding cross-sections of stereotactic Atlas of the Rat Brain are provided for reference in the left.

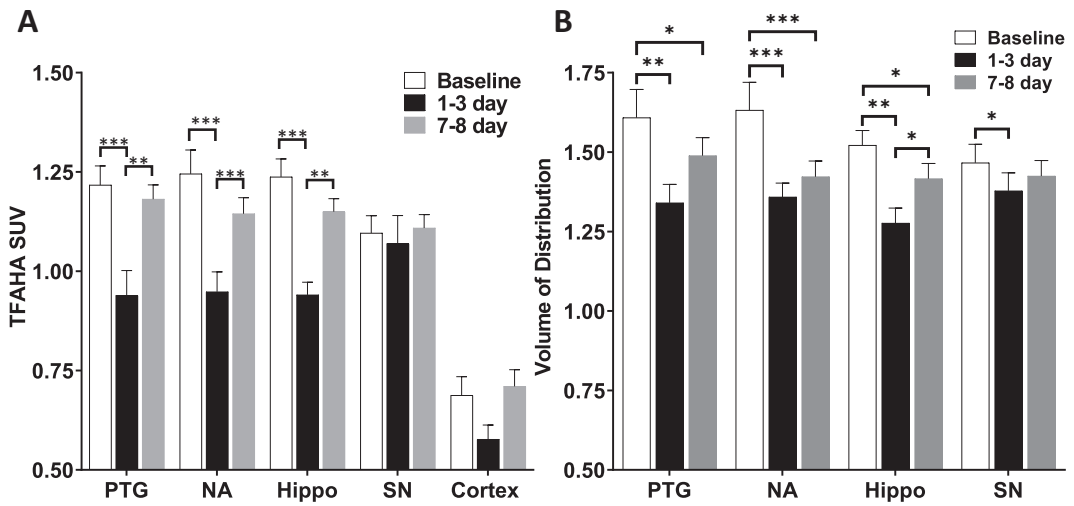

Fig. 2 Changes in [^{18}F]TFAHA accumulation in different structures of the rat brain at baseline and different days post TBI in *peri-3rd ventricular thalamic gray matter (PTG), n. accumbens, hippocampus*, and *substantia nigra*. **A** SUV and **B** volumes of distribution (VD). Data are mean ± SEM. Statistical significance was determined via one-way ANOVA for repeated measures: *$p < 0.05$, **$p < 0.01$, ***$p < 0.001$.

HDAC5 expression in neurons

At baseline, higher levels of HDAC5 expression were observed in neurons of the *hippocampus*, *peri-3rd ventricular thalamus*, and *n. accumbens*, as compared to neurons in other examined regions of the brain (Figs. 4, 5, and S16). The intracellular localization of HDAC5 in neurons of these regions was both nuclear and cytoplasmic (dual), as evidenced by the comparable percentages of nuclear-only and dual-stained neurons (Fig. S19), as well as by the cytoplasmic-to-nuclear OD ratio close to 1 (Fig. 6B). Notably high levels of HDAC5 were localized in the thalamus close to the 3rd ventricle neuropil (Fig. 4). During the 1–3 days post mTBI, the overall level of HDAC5 expression in neurons in these few regions was significantly reduced (Figs. 4, 5, and S16), while the intracellular localization of HDAC5 expression was shifted predominantly to the perinuclear cytoplasmic region, as evidenced by the significantly increased ($p < 0.05$) percentage of only cytoplasm-stained neurons (Fig. S19) and increased perinuclear cytoplasmic-to-nuclear OD (Fig. 6B), as compared to baseline levels. Notably, the axonal (neuropil) localization of HDAC5 was diminished during the 1–3 days post mTBI (Fig. 4). During the 7–8 days post mTBI, the overall level of HDAC5 expression in neurons remained lower than baseline but showed a tendency to increase over the levels observed at 1–3 days post mTBI (Figs. 4, 5, and S16). However, the subcellular localization of HDAC5

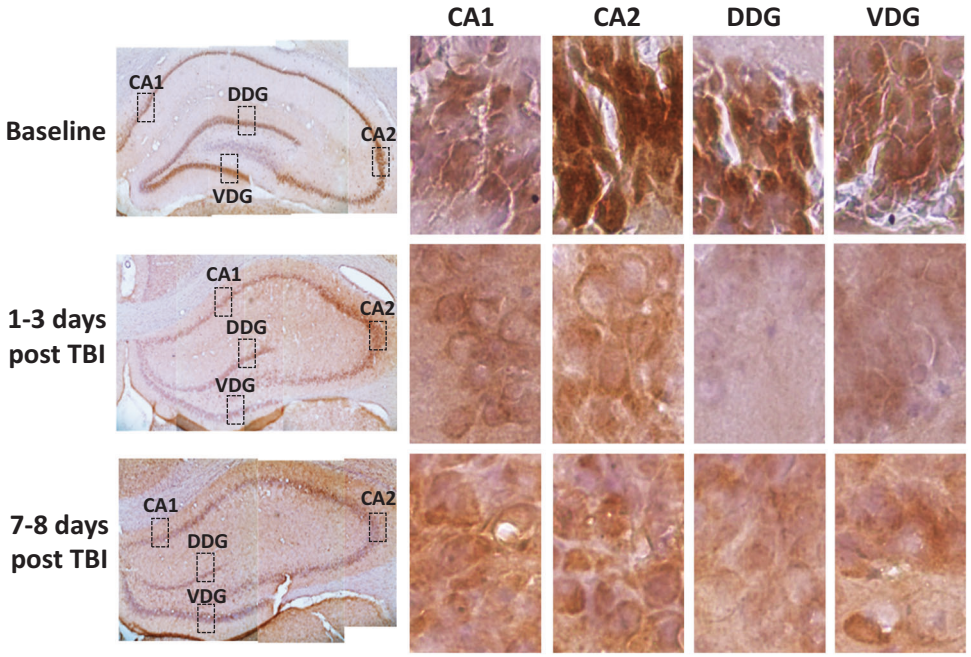

Fig. 3 Expression of HDAC4 in the rat *hippocampus* at baseline, 1–3 days, and 7–8 days post-TBI, visualized by IHC. Left column: stitched images (×10 magnification) with black rectangles indicating hippocampal CA1, CA2, dorsal dentate gyrus (DDG), and ventral dentate gyrus (VDG) areas shown in the corresponding ×40 magnification.

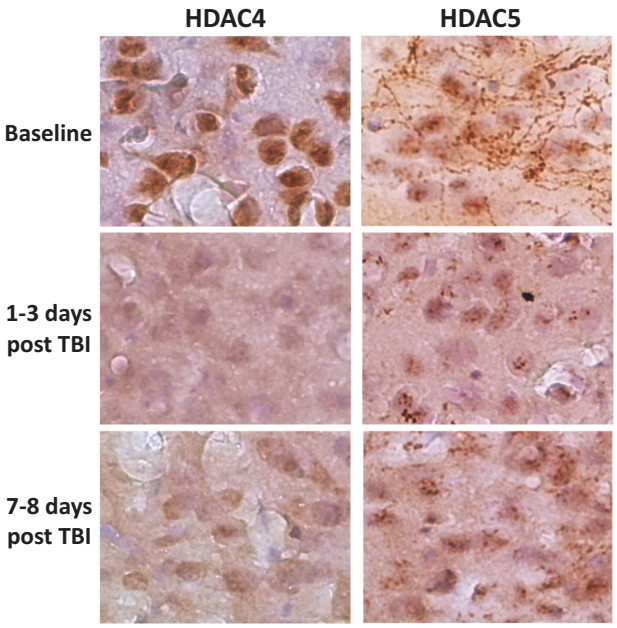

Fig. 4 Expression of HDAC4 and HDAC5 in the paraventricular thalamic nucleus in the rat brain. IHC staining of the brain tissue sections for HDAC4 and HDAC5 was performed at baseline, 1-3 days, and 7-8 days post mTBI. Images are at x40 magnification.

expression at 7–8 days post mTBI was further shifted to the perinuclear cytoplasm, as evidenced by the significantly increased ($p < 0.05$) percentage of only cytoplasm-stained neurons (Fig. S19) and increased perinuclear cytoplasmic-to-nuclear OD (Fig. 6B), as compared to baseline ($p < 0.05$); the axonal (neuropil) localization of HDAC5 showed a tendency to increase as compared to 1–3 days post mTBI (Fig. 4). These pathological changes were not found in other regions of the brain.

DISCUSSION

TBI causes abnormalities in cellular signaling, morphology, and function, as well as reactive-adaptive responses in neurons, glia, and microvasculature [12–14]. In this study, we used the well-established "Marmarou model" of mTBI [47–52], which is known to cause diffuse axonal injury without focal contusion and hemorrhagic lesions. Current histological and immunohistochemical analyses of brain tissue of rats subjected to this mTBI model demonstrate as early as at 6 h post-trauma the upregulation of biomarkers of neuronal stress and neuronal damage (i.e., HSP70, APP, CB2), as well as biomarkers of reactive microglial activation (i.e., IBA1), both in the hippocampus and a few additional brain regions. These results are in agreement with several previous reports from our group and others that have also used this model of mTBI. For example, an increase in HSP70 expression in the CA1 region of the rat hippocampus was previously observed as early as 12 h post-trauma [73]. The HSP70 binds to inflammatory transcription factors, prevents neuronal cell death and neuroinflammation, and reduces brain lesion size and hemorrhage post-TBI [74, 75]. The overexpression of HSP70 inhibits the aggregation of proteins and protects from neurodegeneration in TBI and ischemic reperfusion injury [76, 77]. Increased accumulation of beta-amyloid precursor protein (β-APP) in this mTBI model has been previously reported by us in traumatized neuronal axons of the pyramidal tract and *corpus callosum* [78], and the magnitude of β-APP expression correlated with the linear acceleration of the injury-inducing impactor [51, 52]. The latter is due to interruption of axonal transport caused by diffuse axonal injury, swelling of axonal bulbs, ultimately leading to neuronal cell death, as shown by us [51, 52, 78] and others [79]. Similar to our current experimental findings, other reports demonstrated an increased accumulation of APP in the hippocampus (predominantly in the CA3 region) and in the cerebral cortex during the acute phase post mTBI [73, 76, 80]. The results of these studies in rats are highly relevant to human patients with diffuse axonal injury of the brain because the APP accumulation was observed in damaged axons in the human cortex within a few hours after trauma [45, 81, 82]. As previously shown in a murine TBI model, the cannabinoid receptor

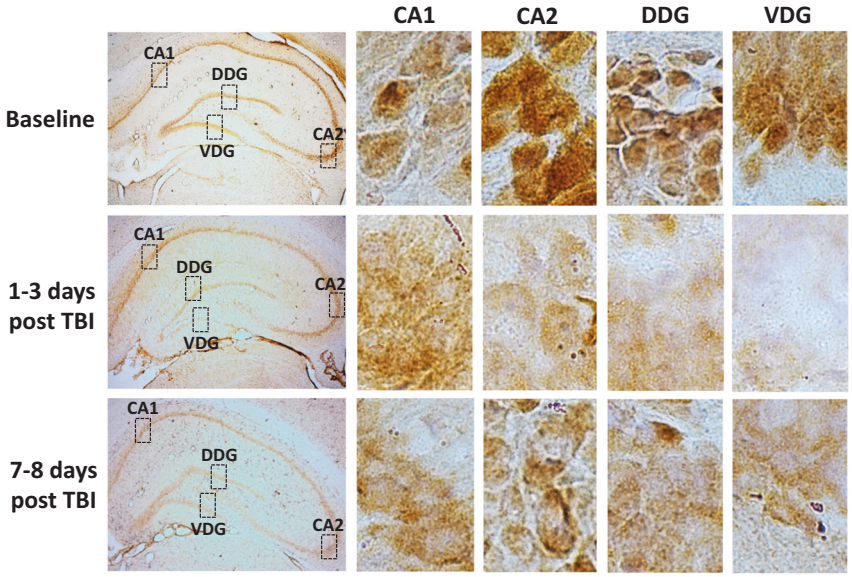

Fig. 5 Expression of HDAC5 in the rat *hippocampus* at baseline, 1–3 days, and 7-8 days post-TBI, visualized by IHC. Left column: stitched images (×5 magnification) with black rectangles indicating hippocampal CA1, CA2, dorsal dentate gyrus (DDG), and ventral dentate gyrus (VDG) areas shown in the corresponding images at ×40 magnification.

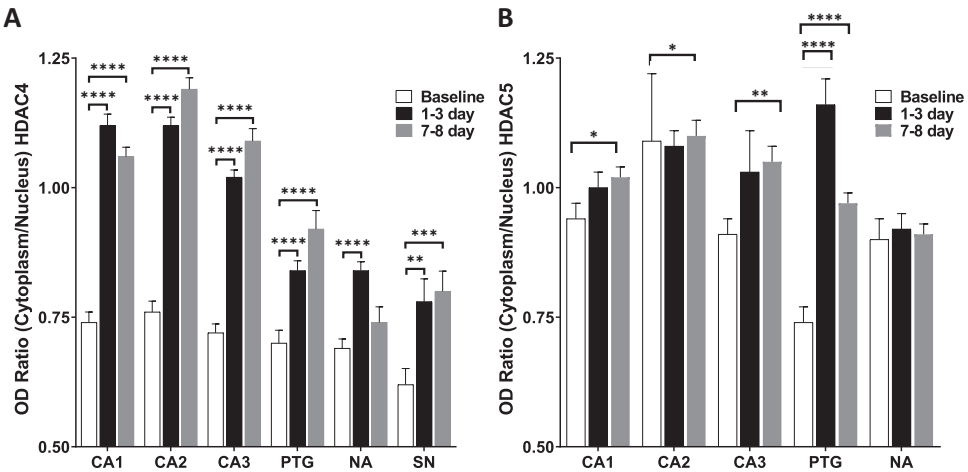

Fig. 6 The ratio of cytoplasmic vs nuclear localization/expression levels of HDAC4 and HDAC5 in different structures of the rat brain. Measurements were obtained by optical densitometry of immunohistochemically stained brain tissue sections from different animals at baseline, 1–3 days, and 7–8 days post-TBI for **A** HDAC4 and **B** HDAC5. Data are mean ± SEM. Statistical significance was determined via one-way ANOVA for repeated measures. *$p < 0.05$, **$p < 0.01$, ***$p < 0.001$.

type 2 (CB2) is up-regulated in activated microglia and astrocytes [83]. Activation of CB2 in the brain after trauma reduces neuroinflammation by downregulation of nitric oxide production, caspase-3 expression [84], and NF-κβ pathway [85] activity, and also by inducing the mitogen-activated protein kinase phosphatase-1 (MPK-1) in reactive microglial cells [86]. Early activation of microglia is one of the hallmarks of diffuse axonal brain injury induced by this mTBI model [87, 88]. Similar to our current observations, the upregulation of IBA1- a biomarker of activated microglia [89–92] has been observed in the microglial cells of hippocampus as early as 6 h post mTBI [88]. Thus, the results of our study confirm the validity of the mTBI model for studying the roles of HDACs class IIa in the setting of epigenetic regulation of reactive and/or adaptive cellular responses to mTBI.

By using non-invasive, repetitive, quantitative in vivo PET/CT imaging with [^{18}F]TFAHA we have demonstrated that during acute (1–3 days) and subacute (7-8 days) phases post mTBI, the level of expression-activity of HDACs class IIa is downregulated in several structures of the rat brain, including the *hippocampus, n. accumbens, peri-3rd ventricle thalamus*, and *substantia nigra*. We observed similar trends in HDACs class IIa expression-activity by PET imaging between 1 and 3 days post mTBI versus baseline. Pooling the data for 1 and 3 days post-injury has increased the statistical significance of differences between the acute phase post-injury versus baseline. The results of in vivo PET/CT imaging have been confirmed by IHC analysis of HDAC4 and HDAC5 expression in the brain tissue sections obtained from a separate group of rats that have been subjected to mTBI and sacrificed during the same period post mTBI. These findings are in agreement with a previous report [44] that mTBI induced by a controlled cortical impact causes a downregulation of HDAC4 activity at 72 h post mTBI. The mechanism of downregulation of HDAC4 expression-activity following mTBI involves the activation of GSK3*β*, which phosphorylates the serine 298 residue of the proline (P), glutamic acid (E), serine (S), threonine (T) domain of HDAC4 (termed PEST) and targets it for degradation, while

treatment with lithium (a known inhibitor of GSK3β) prevents the phosphorylation of HDAC4 and rescues the loss of HDAC4 following mTBI [44]. Furthermore, the latter study has also shown that the loss of HDAC4 causes aberrant activation of Pax3-Ngn2 signaling pathway and the over-production of vGlut1 in hippocampal glutamatergic neurons, and disrupts the balance between glutamatergic and GABAergic neuronal activity after mTBI. The excess glutamate resulting from this cascade can, among other effects, influence neuronal differentiation. Another notable finding in that study was that the overexpression of HDAC4 in the hippocampus by plasmid-mediated transfection prior to mTBI restores neurogenesis, reduces anxiety and depression-like behavior, improves memory functions, and prevents PTSD [44].

In contrast, another recent report [45] applying a weight drop model of repeated mTBI in rats has demonstrated that the compromised hippocampal recognition memory was associated with an upregulation of hippocampal HDAC4 and HDAC5 mRNA levels, as well as hypoacetylation of histones during both, 48 h and 30 days post mTBI. The latter study has also demonstrated that treatment with TSA led to recovered hippocampal learning and memory deficit. However, the apparent differences with the results of our current study can presumably be reconciled, at least in part, by contrasting the different methodologies used for the assessment of expression and activity of HDAC4 and 5. In our current study, we quantified the levels of expression-activity of HDACs class IIa in vivo by using PET/CT with [^{18}F]TFAHA, which accounts for both, the HDACs class IIa expression at the protein (enzyme) level, as well as the level of enzyme activity. It has been well-established that the levels of activity of HDAC4 and HDAC5 depend on post-translational modifications, such as phosphorylation of different domains causing different physiopathological consequences (i.e., activation, nuclear export [93], degradation [94]), and/or the formation of complexes with other proteins and other HDAC isoforms (i.e., HDAC4/MEF2 [95], HDAC4/NCoR/HDAC3 [96]), as well as several other known factors affecting HDACs class IIa activity within the intracellular microenvironment [97]. Measurements of HDAC mRNA levels neither accurately determine HDACs expression at the protein level nor reflect their functional complex formation and enzymatic activity, which depends largely on their post-translational modifications affecting their stability and degradation rates. One should point out that the IHC staining of tissue sections and Western blot analysis can yield semi-quantitative measures of expression of HDACs at the protein level, but they do not provide information about their acetyl-lysine recognition or active complex-forming status (i.e., HDAC4/NCoR/HDAC3 [98]). Thus, the reported upregulation of HDAC4 mRNA expression following repetitive TBI [45] may be effectively countered by increased degradation of HDAC4 induced by phosphorylation of its PEST domain by GSK3β, which is up-regulated in TBI [44]. Therefore, the mechanism of post-transcriptional regulation of HDAC4 expression-activity in mTBI requires further detailed investigation.

Furthermore, it is important to note that not only the level of expression-activity but also the subcellular localization of HDAC4 and HDAC5 are equally important in the molecular pathophysiology of mTBI. This is because nuclear versus cytoplasmic localization of HDAC4 and HDAC5 targets different signaling proteins and transcription factors. For example, in the murine model of neuronal ataxia-telangiectasia deficiency, the increased dephosphorylation of HDAC4 leads to its nuclear accumulation, binding to MEF2A and CREB, and repressing transcriptional activity, which causes neurodegeneration [99]. Similarly, in dopaminergic neurons overexpressing A53T α-synuclein mutation, treatment with 1-methyl-4-phenyl-1,2,3,6-tetrahydropyridine induces oxidative stress, increases interactions of HDAC4 and PP2A, thereby resulting in nuclear accumulation of HDAC4 and transcriptional repression of MEF2A and CREB, which in turn may trigger degeneration of dopaminergic neurons, Parkinson's disease, and dementia [100]. Moreover, it has been demonstrated that the large influx of ionized calcium into neurons after TBI leads to activation of calcium/calmodulin-dependent protein kinases (CaMKI, CaMKII, and CaMKIV) in the CA1, CA3, and dentate gyrus regions of the hippocampus and causes hippocampal-dependent memory loss [101]. Numerous calcium-dependent protein kinases, including CaMKs, phosphorylate three conserved serine residues in the N-terminal regulatory domain of class IIa HDAC species [102–107]. Phosphorylation creates docking sites for the 14-3-3 chaperone protein, which binds phosphorylated HDACs and escorts them from the nucleus to the cytoplasm, relieving downstream transcription factors, such as MEF2, from their repressive influence [108–110]. Phosphorylation by CaMKII requires docking of the kinase to a specific domain of HDAC4 not present in other HDACs and promotes the nuclear export of other class IIa HDACs, such as HDAC5, which does not bind the CaMKII directly [111]. The HDAC4 and HDAC5 form homo- and hetero-oligomers via a conserved coiled-coil domain near their amino-termini. Whereas HDAC5 alone is unresponsive to CaMKII, it becomes responsive to CaMKII in the presence of HDAC4. The acquisition of CaMKII responsiveness by HDAC5 is mediated by the direct association of HDAC5 to HDAC4 and can occur either by phosphorylation of HDAC4 or by transphosphorylation by CaMKII bound to HDAC4. HDAC4 integrates upstream Ca^{2+}-dependent signals via its association with CaMKII and transmits these signals to HDAC5 by protein-protein interactions. Therefore, HDAC4 represents a focal point of convergence for CaMKII signaling to downstream HDAC-regulated genes, and modulation of the interaction of CaMKII and HDAC4 acts as a means of regulating CaMKII-dependent gene programs [112]. Also, it has been demonstrated that CaMKII is a direct upstream kinase of GSK3β, the activation of which is responsible for neuronal cell death post TBI [113]. Hence, mTBI-induced activation of CaMKs and phosphorylation of HDAC4 may explain, at least in part, the predominantly cytoplasmic localization of HDAC4, while the CAMK-mediated phosphorylation and activation of GSK3β results in GSK3β-induced degradation of HDAC4. In another line of independent investigation, it has been shown that the upregulation of GSK3β activity can lead to hyperphosphorylation of tau protein, which may lead to amyloid-β toxicity resulting in the potential development of Alzheimer's disease [114].

The importance of HDACs class IIa, especially HDAC4 and HDAC5, in normal neuronal differentiation and function has been demonstrated in numerous investigations. HDAC4 acts as a neuroprotective protein across different types of neurons, opposing death-inducing stimuli [115]. The deletion of HDAC4 in the forebrain of the mouse leads to impairment of memory, hippocampal-dependent behavioral learning, and long-term synaptic plasticity. Brain-specific HDAC4 knock-out mice exhibit impairment in motor coordination [37]; indeed, a truncated form of HDAC4 results in defective spatial and memory learning in mice, which translates to mental retardation in humans [116].

HDAC5 is central for axonal function and regeneration post brain trauma [117]. In the current study, a decrease of HDAC5 levels in the thalamic neuropil was observed during the first week post mTBI, which is due to impaired axonal transport caused by diffuse axonal injury [38]. These observations are central for the understanding of mechanisms of memory loss and neurodegeneration resulting from brain trauma and may increase the risk of neurodegenerative disease development. Previously, it has been reported that the loss of HDAC5 leads to impaired spatial and associative memory function in a mouse model of Alzheimer's disease [118]. A recent study demonstrated that the pharmacologic inhibition of HDAC5 by using MC1568 in dopaminergic neurons in the *substantia nigra* can help in immature neurite growth by nuclear export of HDAC5, which promotes the upregulation of BMP2 and BMP-signaling pathways [119]. The cytoplasmic localization of HDAC5 prevents the accumulation of

α-synuclein-induced neurodegeneration and the development of Parkinson's disease after mTBI [119, 120].

The results of current studies and those reported by Saha et al. [44] support the rationale for the development of therapeutic strategies to upregulate the expression and activity of HDACs class IIa post-TBI. Although the neuroprotective efficacy of TSA has been previously demonstrated in a rat model of repetitive mTBI [45], TSA is a predominant HDAC class I and IIb inhibitor, with very little inhibitory activity against HDAC4 and 5 [36]. Therefore, the improvement in hippocampal learning and memory deficit in TSA-treated mice subjected to repetitive mTBI can be largely attributed to the well-established neuroprotective effects resulting from the inhibition of HDACs class I and IIb [121, 122]. In addition to lithium chloride, other more specific inhibitors of GSK3β (i.e., Tedeglusib, LY2090314, 9-ING-41 [123]) and CaMKII inhibitors (i.e., KN-62 [124, 125]) should be investigated in mTBI, because these drugs can inhibit the CAMK-GSK3β-induced nuclear export and degradation of HDACs class IIa. Also, the HDAC class IIa-specific inhibitors (i.e., MC1568 [126, 127] and tasquinimod [69, 98, 128]) should be used to investigate the impact of pharmacological inhibition of HDAC class IIa activity and complexation with HDAC class I on the neuro-behavioral outcomes of mTBI.

One of the limitations of the current study is the lack of repetitive MRI for the detection and monitoring of pathomorphological changes in the brain of rats following mTBI (i.e., BBB integrity, brain edema). Unfortunately, the complexity of logistics and scheduling of repetitive imaging experiments have precluded us from the addition of MRI to PET/CT in this particular study. Such type of studies can be greatly facilitated by PET/MRI hybrid instrument for small animal imaging, which is currently not available at our institution. Nevertheless, previously we have conducted repetitive MRI and comparative pathomorphological studies in this model of mTBI and reported the results elsewhere [53, 129]. Also, studies by Marmarou's group using repetitive MRI in this closed impact model of mTBI have demonstrated the lack of persistent BBB disruption and predominantly cytotoxic nature of brain edema during the first 1–4 h [58, 130] and the following 2 weeks post mTBI [131, 132].

In summary, a diffuse mTBI in adult rats is associated with downregulation and predominantly perinuclear cytoplasmic translocation of HDACs class IIa expression and activity in the *hippocampus, n. accumbens, peri-3rd ventricular thalamic gray matter*, and *substantia nigra*. Taken together with numerous previous reports of the importance of HDACs class IIa in neurogenesis, neuronal differentiation, and function, the results of our current study, provide a strong rationale for the development of therapeutic strategies towards upregulation of the expression-activity of HDACs class IIa in the brain post-TBI. Non-invasive molecular imaging with PET/CT (MRI) with [^{18}F] TFAHA can facilitate the pre-clinical development and clinical translation of specific therapeutic approaches to upregulate the expression and activity of HDACs class IIa enzymes in the brain after TBI.

REFERENCES

1. Peterson AB, Xu L, Daugherty J, Breiding MJ. Surveillance report of traumatic brain injury-related emergency department visits, hospitalizations, and deaths. Center for Disease Control and Prevention; United States: U.S. Department of Health and Human Services, 2019.
2. Hammond FM, Giacino JT, Nakase Richardson R, Sherer M, Zafonte RD, Whyte J, et al. Disorders of consciousness due to traumatic brain injury: functional status ten years post-injury. J Neurotrauma. 2019;36:1136–46.
3. Holzer KJ, Carbone JT, DeLisi M, Vaughn MG. Traumatic brain injury and coextensive psychopathology: New evidence from the 2016 Nationwide Emergency Department Sample (NEDS). J Psychiatry Res. 2019;114:149–52.
4. MacGregor AJ, Dougherty AL, Galarneau MR. Injury-specific correlates of combat-related traumatic brain injury in operation Iraqi freedom. J Head Trauma Rehabil. 2011;26:312–18.
5. Rigg JL, Mooney SR. Concussions and the military: Issues specific to service members. PMR. 2011;3:S380–6.
6. Hoge CW, McGurk D, Thomas JL, Cox AL, Engel CC, Castro CA. Mild traumatic brain injury in U.S. soldiers returning from Iraq. N Engl J Med. 2008;358:453–63.
7. Schneiderman AI, Braver ER, Kang HK. Understanding sequelae of injury mechanisms and mild traumatic brain injury incurred during the conflicts in Iraq and Afghanistan: persistent postconcussive symptoms and posttraumatic stress disorder. Am J Epidemiol. 2008;167:1446–52.
8. Kennedy JE, Leal FO, Lewis JD, Cullen MA, Amador RR. Posttraumatic stress symptoms in OIF/OEF servicemembers with blast-related and non-blast-related mild TBI. NeuroRehabilitation. 2010;26:223–31.
9. Hill JJ, Mobo BHP, Cullen MR. Separating deployment-related traumatic brain injury and posttraumatic stress disorder in veterans: preliminary findings from the Veterans Affairs traumatic brain injury screening program. Am J Phys Med Rehabil. 2009;88:605–14.
10. Carlson KF, Nelson D, Orazem RJ, Nugent S, Cifu DX, Sayer NA. Psychiatric diagnoses among Iraq and Afghanistan war veterans screened for deployment-related traumatic brain injury. J Trauma Stress. 2010;23:17–24.
11. Belanger HG, Uomoto JM, Vanderploeg RD. The veterans health administration system of care for mild traumatic brain injury: costs, benefits, and controversies. J Head Trauma Rehabil. 2009;24:4–13.
12. Chodobski A, Zink BJ, Szmydynger-Chodobska J. Blood-brain barrier pathophysiology in traumatic brain injury. Transl Stroke Res. 2011;2:492–516.
13. Hemphill MA, Dauth S, Yu CJ, Dabiri BE, Parker KK. Traumatic brain injury and the neuronal microenvironment: A potential role for neuropathological mechanotransduction. Neuron. 2015;85:1177–92.
14. VSSS Sajja, Hlavac N, VandeVord PJ. Role of glia in memory deficits following traumatic brain injury: Biomarkers of glia dysfunction. Front Integr Neurosci. 2016;10:7.
15. Wong VS, Langley B. Epigenetic changes following traumatic brain injury and their implications for outcome, recovery and therapy. Neurosci Lett. 2016;625:26–33.
16. Shein NA, Shohami E. Histone deacetylase inhibitors as therapeutic agents for acute central nervous system injuries. Mol Med. 2011;17:448–56.
17. Kiefer JC. Epigenetics in development. Dev Dyn. 2007;236:1144–56.
18. Reik W, Dean W, Walter J. Epigenetic reprogramming in mammalian development. Science. 2001;293:1089–93.
19. Majdzadeh N, Morrison BE, D'Mello SR. Class IIA HDACs in the regulation of neurodegeneration. Front Biosci. 2008;13:1072–82.
20. Seto E, Yoshida M. Erasers of histone acetylation: The histone deacetylase enzymes. Cold Spring Harb Perspect Biol. 2014;6:a018713, 1–26.
21. Qureshi IA, Mehler MF. Understanding neurological disease mechanisms in the era of epigenetics. JAMA Neurol. 2013;70:703–10.
22. Hahnen E, Hauke J, Tränkle C, Eyüpoglu IY, Wirth B, Blümcke I. Histone deacetylase inhibitors: possible implications for neurodegenerative disorders. Expert Opin Investig Drugs. 2008;17:169–84.
23. Jin K, Mao XO, Simon RP, Greenberg DA. Cyclic AMP response element-binding protein (CREB) and CREB binding protein (CBP) in global cerebral ischemia. J Mol Neurosci. 2001;16:49–56.
24. Rouaux C, Jokic N, Mbebi C, Boutillier S, Loeffler JP, Boutillier AL. Critical loss of CBP/p300 histone acetylase activity by caspase-6 during neurodegeneration. EMBO J. 2003;22:6537–49.
25. Gibson CL, Murphy SP. Benefits of histone deacetylase inhibitors for acute brain injury: A systematic review of animal studies. J Neurochem. 2010;115:806–13.
26. Dash PK, Orsi SA, Zhang M, Grill RJ, Patil S, Zhao J, et al. Valproate administered after traumatic brain injury provides neuroprotection and improves cognitive function in rats. PLoS ONE. 2010;5:e11383, 1–13.
27. Kozikowski AP, Chen Y, Gaysin A, Chen B, D'Annibale MA, Suto CM, et al. Functional differences in epigenetic modulators - Superiority of mercaptoacetamide-based histone deacetylase inhibitors relative to hydroxamates in cortical neuron neuroprotection studies. J Med Chem. 2007;50:3054–61.
28. Zhang B, West EJ, Van KC, Gurkoff GG, Zhou J, Zhang XM, et al. HDAC inhibitor increases histone H3 acetylation and reduces microglia inflammatory response following traumatic brain injury in rats. Brain Res. 2008;1226:181–91.
29. Nikolian VC, Dennahy IS, Weykamp M, Williams AM, Bhatti UF, Eidy H, et al. Isoform 6-selective histone deacetylase inhibition reduces lesion size and brain swelling following traumatic brain injury and hemorrhagic shock in. J Trauma Acute Care Surg. 2019;86:232–9.
30. Golay J, Cuppini L, Leoni F, Micò C, Barbui V, Domenghini M, et al. The histone deacetylase inhibitor ITF2357 has anti-leukemic activity in vitro and in vivo and inhibits IL-6 and VEGF production by stromal cells. Leukemia. 2007;21:1892–1900.
31. Shein NA, Grigoriadis N, Alexandrovich AG, Simeonidou C, Lourbopoulos A, Polyzoidou E, et al. Histone deacetylase inhibitor ITF2357 is neuroprotective,

improves functional recovery, and induces glial apoptosis following experimental traumatic brain injury. FASEB J. 2009;23:4266–75.
32. Yang H, Ni W, Jiang H, Lei Y, Su J, Gu Y, et al. Histone deacetylase inhibitor Scriptaid alleviated neurological dysfunction after experimental intracerebral hemorrhage in mice. Behav Neurol. 2018;2018:6583267. https://doi.org/10.1155/2018/6583267.
33. Wang G, Shi Y, Jiang X, Leak RK, Hu X, Wu Y, et al. HDAC inhibition prevents white matter injury by modulating microglia/macrophage polarization through the GSK3β/PTEN/Akt axis. Proc Natl Acad Sci USA. 2015;112:2853–8.
34. Wang G, Jiang X, Pu H, Zhang W, An C, Hu X, et al. Scriptaid, a novel histone deacetylase inhibitor, protects against traumatic brain injury via modulation of PTEN and AKT pathway: scriptaid protects against TBI via AKT. Neurotherapeutics. 2013;10:124–42.
35. Lu J, Frerich JM, Turtzo LC, Li S, Chiang J, Yang C, et al. Histone deacetylase inhibitors are neuroprotective and preserve NGF-mediated cell survival following traumatic brain injury. Proc Natl Acad Sci USA. 2013;110:10747–52.
36. Gaub P, Tedeschi A, Puttagunta R, Nguyen T, Schmandke A, Di Giovanni S. HDAC inhibition promotes neuronal outgrowth and counteracts growth cone collapse through CBP/p300 and P/CAF-dependent p53 acetylation. Cell Death Differ. 2010;17:1392–408.
37. Levenson JM, Sweatt JD. Epigenetic mechanisms in memory formation. Nat Rev Neurosci. 2005;6:108–18.
38. Vecsey CG, Hawk JD, Lattal KM, Stein JM, Fabian SA, Attner MA, et al. Histone deacetylase inhibitors enhance memory and synaptic plasticity via CREB: CBP-dependent transcriptional activation. J Neurosci. 2007;27:6128–40.
39. Bradner JE, West N, Grachan ML, Greenberg EF, Haggarty SJ, Warnow T, et al. Chemical phylogenetics of histone deacetylases. Nat Chem Biol. 2010;6:238–43.
40. Kim MS, Akhtar M, Adachi M, Mahgoub M, Bassel-Duby R, Kavalali ET, et al. An essential role for histone deacetylase 4 in synaptic plasticity and memory formation. J Neurosci. 2012;32:10879–86.
41. Cho Y, Sloutsky R, Naegle KM, Cavalli V. Injury-Induced HDAC5 nuclear export is essential for axon regeneration. Cell. 2013;155:894.
42. Sando R, Gounko N, Pieraut S, Liao L, Yates J, Maximov A. HDAC4 governs a transcriptional program essential for synaptic plasticity and memory. Cell. 2012;151:821–34.
43. Agis-Balboa RC, Pavelka Z, Kerimoglu C, Fischer A. Loss of HDAC5 impairs memory function: Implications for Alzheimer's disease. J Alzheimer's Dis. 2013;33:35–44.
44. Saha P, Gupta R, Sen T, Sen N. Histone deacetylase 4 downregulation elicits post-traumatic psychiatric disorders through impairment of neurogenesis. J Neurotrauma. 2019;36:3284–96.
45. Sagarkar S, Balasubramanian N, Mishra S, Choudhary AG, Kokare DM, Sakharkar AJ. Repeated mild traumatic brain injury causes persistent changes in histone deacetylase function in hippocampus: implications in learning and memory deficits in rats. Brain Res. 2019;1711:183–92.
46. Bonomi R, Mukhopadhyay U, Shavrin A, Yeh HH, Majhi A, Dewage SW, et al. Novel histone deacetylase class IIa selective substrate radiotracers for PET imaging of epigenetic regulation in the brain. PLoS ONE. 2015;10:e0133512, 1–19.
47. Abd-Elfattah Foda MA, Marmarou A. A new model of diffuse brain injury in rats. Part II: Morphological characterization. J Neurosurg. 1994;80:301–13.
48. Cernak I. Animal models of head trauma. NeuroRx. 2005;2:410–22.
49. Bodnar CN, Roberts KN, Higgins EK, Bachstetter AD. A systematic review of closed head injury models of mild traumatic brain injury in mice and rats. J Neurotrauma. 2019;36:1683–706.
50. Folkerts MM, Berman RF, Muizelaar JP, Rafols JA. Disruption of MAP-2 immunostaining in rat hippocampus after traumatic brain injury. J Neurotrauma. 1998;15:349–63.
51. Kallakuri S, Cavanaugh JM, Özaktay AC, Takebayashi T. The effect of varying impact energy on diffuse axonal injury in the rat brain: a preliminary study. Exp Brain Res. 2003;148:419–24.
52. Li Y, Zhang L, Kallakuri S, Zhou R, Cavanaugh JM. Quantitative relationship between axonal injury and mechanical response in a Rodent head impact acceleration model. J Neurotrauma. 2011;28:1767–82.
53. Kallakuri S, Bandaru S, Zakaria N, Shen Y, Kou Z, Zhang L, et al. Traumatic brain injury by a closed head injury device induces cerebral blood flow changes and microhemorrhages. J Clin Imaging Sci. 2015;5:52.
54. Li Y, Zhang L, Kallakuri S, Cohen A, Cavanaugh JM. Correlation of mechanical impact responses and biomarker levels: a new model for biomarker evaluation in TBI. J Neurol Sci. 2015;359:280–6.
55. Zakaria N, Kallakuri S, Bandaru, Cavanaugh JM. Temporal assessment of traumatic axonal injury in the rat corpus callosum and optic chiasm. Brain Res. 2012;1467:81–90.
56. Li Y, Zhang L, Kallakuri S, Zhou R, Cavanaugh JM. Injury predictors of traumatic axonal injury in a rodent head impact acceleration model. Stapp Car Crash J. 2011;55:25–47.
57. Li Y, Zhang L, Kallakuri S, Zhou R, Cvanaugh JM. Quantitative relationship between axonal injury and mechanical response in a rodent head impact acceleration model. J Neurotrauma. 2011;28:1767–82.
58. Beaumont A, Fatouros P, Gennarelli T, Corwin F, Marmarou A. Bolus tracer delivery measured by MRI confirms edema without blood-brain barrier permeability in diffuse traumatic brain injury. Acta Neurochir Suppl. 2006;96:171–4.
59. Beaumont A, Marmarou C, Marmarou A. The effects of human corticotrophin releasing factor on motor and cognitive deficit after impact acceleration injury. Neurol Res. 2000;22:665–73.
60. Chen X, Chen Y, Xu Y, Gao Q, Shen Z, Zheng W. Microstructural and neurochemical changes in the rat brain after diffuse axonal injury. J Magn Res Imaging. 2019;49:1069–77.
61. Song Y, Qian Y, Su W, Liu X, Huang J, Gong Z, et al. Differences in pathological changes between two rat models of severe traumatic brain injury. Neural Regen Res. 2019;14:1796–804.
62. Li S, Sun Y, Shan D, Feng B, Xing J, Duan Y, et al. Temporal profiles of axonal injury following impact acceleration traumatic brain injury in rats – a comparative study with diffusion tensor imaging and morphological analysis. Int J Leg Med. 2013;127:159–67.
63. Goda M, Isono M, Fujiki M, Kobayashi H. Both MK801 and NBQX reduce the neuronal damage after impact-acceleration brain injury. J Neurotrauma. 2002;19:1445–56.
64. Wang H, Ma Y. Experimental models of traumatic axonal injury. J Clin Neurosci. 2010;17:157–62.
65. Marmarou CR, Prieto R, Taya K, Young HF, Marmarou A. Marmarou weight drop injury model. In: Chen J, Xu ZC, Xu XM, Zhang JH, editors. Animal models of acute neurological injuries. Springer Protocols Handbooks. Totowa, New Jersey, USA: Humana Press; 2009. p. 393–407.
66. Marmarou A, Abd-Elfattah Foda MA, Van den Brink W, Campbell J, Kita H, Demetriadou K. A new model of diffuse brain injury in rats. Part I: Pathophysiology and biomechanics. J Neurosurg. 1994;80:291–300.
67. Guo H, Renaut RA, Chen K. An input function estimation method for FDG-PET human brain studies. Nucl Med Biol. 2007;34:483–92.
68. Watson C, Paxinos G. The rat brain in stereotaxic coordinates. San Diego: Academic Press; 2006.
69. Logan J, Fowler JS, Volkow ND, Wang G, Ding Y, Alexoff DL. Distribution volume ratios without blood sampling from graphical analysis of PET data. J Cereb Blood Flow Metab. 1996;16:834–40.
70. Laws MT, Bonomi RE, Kamal SR, Gelovani DJ, Llaniguez J, Potukutchi S, et al. Molecular imaging HDACs class IIa expression-activity and pharmacologic inhibition in intracerebral glioma models in rats using PET/CT/(MRI) with [^{18}F] TFAHA. Sci Rep. 2019;9:3595.
71. Logan J, Fowler JS, Volkow ND, Wolf AP, Dewey SL, Schlyer DJ. et al. Graphical analysis of reversible radioligand binding from time-activity measurements applied to [N-11C-methyl]-(-)-cocaine PET studies in human subjects. J Cereb Blood Flow Metab.1990;10:740–7.
72. Murakami N, Yamaki T, Iwamoto Y, Sakakibara T, Kobori N, Fushiki S, et al. Experimental brain injury induces expression of amyloid precursor protein, which may be related to neuronal loss in the hippocampus. J Neurotrauma. 1998;15:993–1003.
73. Zhang MH, Zhou XM, Cui JZ, Wang KJ, Feng Y, Zhang HA. Neuroprotective effects of dexmedetomidine on traumatic brain injury: Involvement of neuronal apoptosis and HSP70 expression. Mol Med Rep. 2018;17:8079–86.
74. Kim JY, Kim N, Zheng Z, Lee JE, Yenari MA. The 70 kDa heat shock protein protects against experimental traumatic brain injury. Neurobiol Dis. 2013;58:289–95.
75. Jassam YN, Izzy S, Whalen M, McGavern DB, El Khoury J. Neuroimmunology of traumatic brain injury: Time for a paradigm shift. Neuron. 2017;95:1246–65.
76. Kim N, Kim JY, Yenari MA. Anti-inflammatory properties and pharmacological induction of Hsp70 after brain injury. Inflammopharmacology. 2012;20:177–85.
77. Eroglu B, Kimbler D, Pang J, Choi J, Moskophidis D, Yanasak N, et al. Therapeutic inducers of the HSP70/HSP110 protect mice against traumatic brain injury. J Neurochemistry. 2014;130:626–41.
78. Kallakuri S, Li Y, Zhou R, Bandaru S, Zakaria N, Zhang L, et al. Impaired axoplasmic transport is the dominant injury induced by an impact acceleration injury device: an analysis of traumatic axonal injury in pyramidal tract and corpus callosum of rats. Brain Res. 2012;1452:29–38.
79. Hsieh TH, Kang JW, Lai JH, Huang YZ, Rotenberg A, Chen KY, et al. Relationship of mechanical impact magnitude to neurologic dysfunction severity in a rat traumatic brain injury model. PLoS ONE. 2017;12:e0178186, 1–18.
80. Ciallella JR, Ikonomovic MD, Paljug WR, Wilbur YI, Dixon CE, Kochanek PM, et al. Changes in expression of amyloid precursor protein and interleukin-1β after experimental traumatic brain injury in rats. J Neurotrauma. 2002;19:1555–67.
81. Johnson VE, Stewart W, Smith DH. Axonal pathology in traumatic brain injury. Exp Neurol. 2013;246:35–43.

82. Shishido H, Ueno M, Sato K, Matsumura M, Toyota Y, Kirino T, et al. Traumatic brain injury by weight-drop method causes transient amyloid-β deposition and acute cognitive deficits in mice. Behav Neurol. 2019;2019:3248519. https://doi.org/10.1155/2019/3248519.
83. Elliott MB, Tuma RF, Amenta PS, Barbe MF, Jallo JI. Acute effects of a selective cannabinoid-2 receptor agonist on neuroinflammation in a model of traumatic brain injury. J Neurotrauma. 2011;28:973–81.
84. Chen Y, Buck J. Cannabinoids protect cells from oxidative cell death: a receptor-independent mechanism. J Pharmacol Exp Ther. 2000;293:807–12.
85. Nikodemova M, Duncan ID, Watters JJ. Minocycline exerts inhibitory effects on multiple mitogen-activated protein kinases and IκBα degradation in a stimulus-specific manner in microglia. J Neurochem. 2006;96:314–23.
86. Eljaschewitsch E, Witting A, Mawrin C, Lee T, Schmidt PM, Wolf S, et al. The endocannabinoid anandamide protects neurons during CNS inflammation by induction of MKP-1 in microglial cells. Neuron 2006;49:67–79.
87. Donat CK, Scott G, Gentleman SM, Sastre M. Microglial activation in traumatic brain injury. Front Aging Neurosci. 2017;15:349–63.
88. Madathil SK, Wilfred BS, Urankar SE, Yang W, Leung LY, Shear DA, et al. Early microglial activation following closed-head concussive injury is dominated by pro-inflammatory M-1 type. Front Neurol. 2018;9:964.
89. Jin Y, Wang R, Yang S, Zhang X, Dai J. Role of Microglia autophagy in microglia activation after traumatic brain injury. World Neurosurg. 2017;100:351–60.
90. Imai Y, Kohsaka S. Intracellular signaling in M-CSF-induced microglia activation: role of Iba1. Glia. 2002;40:164–74.
91. Imai Y, Ibata I, Ito D, Ohsawa K, Kohsaka S. A novel gene iba1 in the major histocompatibility complex class III region encoding and EF hand protein expressed in a monocytic lineage. Biochem Biophys Res Commun. 1996;224:855–62.
92. Ito D, Tanaka K, Suzuki S, Dembo T, Fukuuchi Y. Enhanced expression of Iba1, ionized calcium-binding adapter molecule 1, after transient focal cerebral ischemia in rat brain. Stroke. 2001;32:1208–15.
93. Verdin E, Dequiedt F, Kasler HG. Class II histone deacetylases: versatile regulators. Trends Genet. 2003;19:286–93.
94. Cernotta N, Clocchiatti A, Florean C, Brancolini C. Ubiquitin-dependent degradation of HDAC4, a new regulator of random cell motility. Mol Biol Cell. 2011;22:278–89.
95. Bolger TA, Yao TP. Intracellular trafficking of histone deacetylase 4 regulates neuronal cell death. J Neurosci. 2005;25:9544–53.
96. Fischle W, Dequiedt F, Hendzel MJ, Guenther MG, Lazar MA, Verdin E, et al. Enzymatic activity associated with class II HDACs is dependent on a multiprotein complex containing HDAC3 and SMRT/N-CoR. Mol Cell. 2002;9:45–57.
97. Fitzsimons HL. The Class IIa histone deacetylase HDAC4 and neuronal function: Nuclear nuisance and cytoplasmic stalwart? Neurobiol Learn Mem. 2015;123:149–58.
98. Isaacs JT, Antony L, Dalrymple SL, Brennen WN, Gerber S, Leanderson T, et al. Tasquinimod is an allosteric modulator of HDAC4 survival signaling within the compromised cancer microenvironment. Cancer Res. 2013;73:1386–99.
99. Li J, Chen J, Ricupero CL, Hart RP, Schwartz MS, Herrup K, et al. Nuclear accumulation of HDAC4 in ATM deficiency promotes neurodegeneration in ataxia telangiectasia. Nat Med. 2012;18:783–90.
100. Wu Q, Yang X, Zhang L, Zhang Y, Feng L. Nuclear accumulation of histone deacetylase 4 (HDAC4) exerts neurotoxicity in models of Parkinson's disease. Mol Neurobiol. 2017;54:6970–83.
101. Atkins CM, Chen S, Alonso OF, Dietrich WD, Hu BR. Activation of calcium/calmodulin-dependent protein kinases after traumatic brain injury. J Cereb Blood Flow Metab. 2006;26:1507–18.
102. Chang S, Bezprozvannaya S, Li S, Olson EN. An expression screen reveals modulators of class II histone deacetylase phosphorylation. Proc Natl Acad Sci USA. 2005;102:8120–25.
103. Harrison BC, Kim M, van-Rooij E, Plato CF, Papst PJ, McKinsey TA, et al. Regulation of cardiac stress signaling by protein kinase D1. Mol Cell Biol. 2006;26:3875–88.
104. Li X, Song S, Liu Y, Ko SH, Kao HY. Phosphorylation of the histone deacetylase 7 modulates its stability and association with 14-3-3 proteins. J Biol Chem. 2004;279:34201–08.
105. Lehman JJ, Kelly DP. Transcriptional activation of energy metabolic switches in the developing and hypertrophied heart. Clin Exp Pharmacol Physiol. 2002;73:667–77.
106. McKinsey TA, Zhang CL, Lu J, Olson EN. Signal-dependent nuclear export of a histone deacetylase regulates muscle differentiation. Nature. 2000;408:106–11.
107. Vega RB, Harrison BC, Meadows E, Roberts CR, Papst PJ, McKinsey TA, et al. Protein kinases C and D mediate agonist-dependent cardiac hypertrophy through nuclear export of histone deacetylase 5. Mol Cell Biol. 2004;24:8374–85.
108. Grozinger CM, Schreiber SL. Regulation of histone deacetylase 4 and 5 and transcriptional activity by 14-3-3-dependent cellular localization. Proc Natl Acad Sci USA. 2000;97:7835–40.
109. McKinsey TA, Zhang CL, Olson EN. Activation of the myocyte enhancer factor-2 transcription factor by calcium/calmodulin-dependent protein kinase-stimulated binding of 14-3-3 to histone deacetylase 5. Proc Natl Acad Sci USA. 2000;97:14400–5.
110. McKinsey TA, Zhang CL, Olson EN. Identification of a signal-responsive nuclear export sequence in class II histone deacetylases. Mol Cell Biol. 2001;21:6312–21.
111. Backs J, Song K, Bezprozvannaya S, Chang S, Olson EN. CaM kinase II selectively signals to histone deacetylase 4 during cardiomyocyte hypertrophy. J Clin Investig. 2006;116:1853–64.
112. Backs J, Backs T, Bezprozvannaya S, McKinsey TA, Olson EN. Histone deacetylase 5 acquires calcium/calmodulin-dependent kinase II responsiveness by oligomerization with histone deacetylase 4. Mol Cell Biol. 2008;28:3437–45.
113. Song B, Lai B, Zheng Z, Zhang Y, Luo J, Li M, et al. Inhibitory phosphorylation of GSK-3 by CaMKII couples depolarization to neuronal survival. J Biol Chem. 2010;285:41122–34.
114. Xu K, Dai XL, Huang HC, Jiang ZF. Targeting HDACs: a promising therapy for Alzheimer's disease. Oxid Med Cell Longev. 2011;2011:143269. https://doi.org/10.1155/2011/143269.
115. Majdzadeh N, Wang L, Morrison BE, Bassel-Duby R, Olson EN, D'Mello S. HDAC4 inhibits cell-cycle progression and protects neurons from cell death. Dev Neurobiol. 2008;68:1076–92.
116. Sando R, Gounko N, Pieraut S, Liao L, Yates J, Maximov A. HDAC4 governs a transcriptional program essential for synaptic plasticity and memory. Cell. 2012;151:821–34.
117. Cho Y, Cavalli V. HDAC5 is a novel injury-regulated tubulin deacetylase controlling axon regeneration. EMBO J. 2012;31:3063–78.
118. Agis-Balboa RC, Pavelka Z, Kerimoglu C, Fischer A. Loss of HDAC5 impairs memory function: Implications for Alzheimer's disease. J Alzheimer's Dis. 2013;33:35–44.
119. Mazzocchi M, Wyatt SL, Mercatelli D, Morari M, Morales-Prieto N, O'Keeffe GW, et al. Gene Co-expression Analysis identifies histone deacetylase 5 and 9 expression in midbrain dopamine neurons and as regulators of neurite growth via bone morphogenetic protein signaling. Front Cell Dev Biol. 2019;7:191.
120. Cho Y, Sloutsky R, Naegle KM, Cavalli V. Injury-Induced HDAC5 nuclear export is essential for axon regeneration. Cell. 2013;155:894.
121. Vargas-López V, Lamprea MR, Múnera A. Histone deacetylase inhibition abolishes stress-induced spatial memory impairment. Neurobiol Learn Mem. 2016;134:328–38.
122. Levenson JM, O'Riordan KJ, Brown KD, Trinh MA, Molfese DL, Sweatt JD. Regulation of histone acetylation during memory formation in the hippocampus. J Biol Chem. 2004;279:40545–59.
123. Walz A, Ugolkov A, Chandra S, Kozikowski A, Carneiro BA, Mazar AP, et al. Molecular pathways: Revisiting glycogen synthase kinase-3β as a target for the treatment of cancer. Clin Cancer Res. 2017;23:1891–97.
124. Hidaka H, Yokokura H. Molecular and cellular pharmacology of a calcium/calmodulin-dependent protein kinase II (CaM kinase II) Inhibitor, KN-62, and proposal of CaM kinase phosphorylation cascades. Adv Pharmacol. 1996;36:193–219.
125. Tokumitsu H, Chijiwa T, Hagiwara M, Mizutani A, Terasawa M, Hidaka H. KN-62, 1-[N,O-Bis(5-isoquinolinesulfonyl)-N-methyl-L-tyrosyl]−4-phenylpiperazine, a specific inhibitor of Ca^{2+}/calmodulin-dependent protein kinase II. J Biol Chem.1990;265:4315–20.
126. Fleming CL, Ashton TD, Gaur V, McGee SL, Pfeffer FM. Improved synthesis and structural reassignment of MC1568: A class IIa selective HDAC inhibitor. J Med Chem. 2014;57:1132–35.
127. Nebbioso A, Manzo F, Miceli M, Conte M, Manente L, Altucci L, et al. Selective class II HDAC inhibitors impair myogenesis by modulating the stability and activity of HDAC-MEF2 complexes. EMBO Rep. 2009;10:776–82.
128. Raymond E, Dalgleish A, Damber JE, Smith M, Pili R. Mechanisms of action of tasquinimod on the tumour microenvironment. Cancer Chemother Pharmacol. 2014;73:1–8.
129. Benson RR, Gattu R, Sewick B, Kou Z, Zakaria N, Cavanaugh JM, et al. Detection of hemorrhagic and axonal pathology in mild traumatic brain injury using advanced MRI: implications for neurorehabilitation. NeuroRehabilitation. 2012;31:261–79.
130. Beaumont A, Marmarou A, Hayasaki K, Barzo P, Fatouros P, Corwin F, et al. The permissive nature of blood brain barrier (BBB) opening in edema formation following traumatic brain injury. Acta Neurochir Suppl. 2000;76:125–9.
131. Barzo P, Marmarou A, Fatouros P, Hayasaki K, Corwin F. Biphasic pathophysiological response of vasogenic and cellular edema in traumatic brain swelling. Acta Neurochir Suppl. 1997;70:119–22.

132. Barzo P, Marmarou A, Fatouros P, Hayasaki K, Corwin F. Contribution of vasogenic and cellular edema to traumatic brain swelling measure by diffusion-weighted imaging. J Neurosurg. 1997;87:900–7.

ACKNOWLEDGEMENTS

These studies were supported in part by the grants: R01DA042057 (NIDA/NIH) to SP and JGG; and RX002900 (VA) to AC and JGG. The Microscopy, Imaging, and Cytometry Resources Core are supported, in part, by the Cancer Center Support Grant (P30 CA022453, NCI/NIH) to Karmanos Cancer Institute, Wayne State University, Detroit, MI; RP and WA received awards from the Levy-Logenbaugh Donor-Advised Fund.

AUTHOR CONTRIBUTIONS

SRK, RP, WA, RLS, SAP, and JGG designed research; SRK, SP, DJG, RB, SK, and JGG performed research; RB, TM, and JGG contributed new reagents/analytic tools; SRK, SP, DJG, RP, JMC, WA, AC, RLS, SAP, and JGG, analyzed data; SRK, SK, RP, WA, RLS, SAP, and JGG, wrote the paper.

COMPETING INTERESTS

RB and JGG are inventors on issued patents and pending patent applications related to PET imaging of HDACs class IIa expression-activity and are entitled to royalties if licensing or commercialization occurs. Potential conflicts of interest are managed in accordance with established institutional conflict of interest policies of the Wayne State University (Detroit, MI). The other authors declare that no conflicts of interest exist.

ADDITIONAL INFORMATION

Supplementary information The online version contains supplementary material available at https://doi.org/10.1038/s41380-021-01369-7.

Correspondence and requests for materials should be addressed to Juri G. Gelovani.

Reprints and permission information is available at http://www.nature.com/reprints

Publisher's note Springer Nature remains neutral with regard to jurisdictional claims in published maps and institutional affiliations.